

## Article

# Lignocellulosic Biomass as Source for Lignin-Based Environmentally Benign Antioxidants

Abla Alzagameem<sup>1,2</sup>, Basma El Khaldi-Hansen<sup>1</sup>, Dominik Büchner<sup>1</sup>, Michael Larkins<sup>1,3</sup>, Birgit Kamm<sup>2,4</sup>, Steffen Witzleben<sup>1</sup>, Margit Schulze<sup>1\*</sup>

<sup>1</sup> Affiliation 1; Department of Natural Sciences, Bonn-Rhein-Sieg University of Applied Sciences, von-Liebig-Str. 20, D-53359 Rheinbach, Germany; [abla.alzagameem@h-brs.de](mailto:abla.alzagameem@h-brs.de) (A.A.), [basma.elkhaldi-hansen@h-brs.de](mailto:basma.elkhaldi-hansen@h-brs.de) (B.E.K.-H.), [dominik.buechner@h-brs.de](mailto:dominik.buechner@h-brs.de) (D.B.), [steffen.witzleben@h-brs.de](mailto:steffen.witzleben@h-brs.de) (S.W.), [margit.schulze@h-brs.de](mailto:margit.schulze@h-brs.de) (M.S.)

<sup>2</sup> Affiliation 2; Brandenburg University of Technology BTU Cottbus-Senftenberg, Faculty of Environment and Natural Sciences, Platz der Deutschen Einheit 1, D-03046 Cottbus, Germany; [alzagameem@btu-cottbus-senftenberg.de](mailto:alzagameem@btu-cottbus-senftenberg.de); [kamm@btu-cottbus-senftenberg.de](mailto:kamm@btu-cottbus-senftenberg.de) (B.K.)

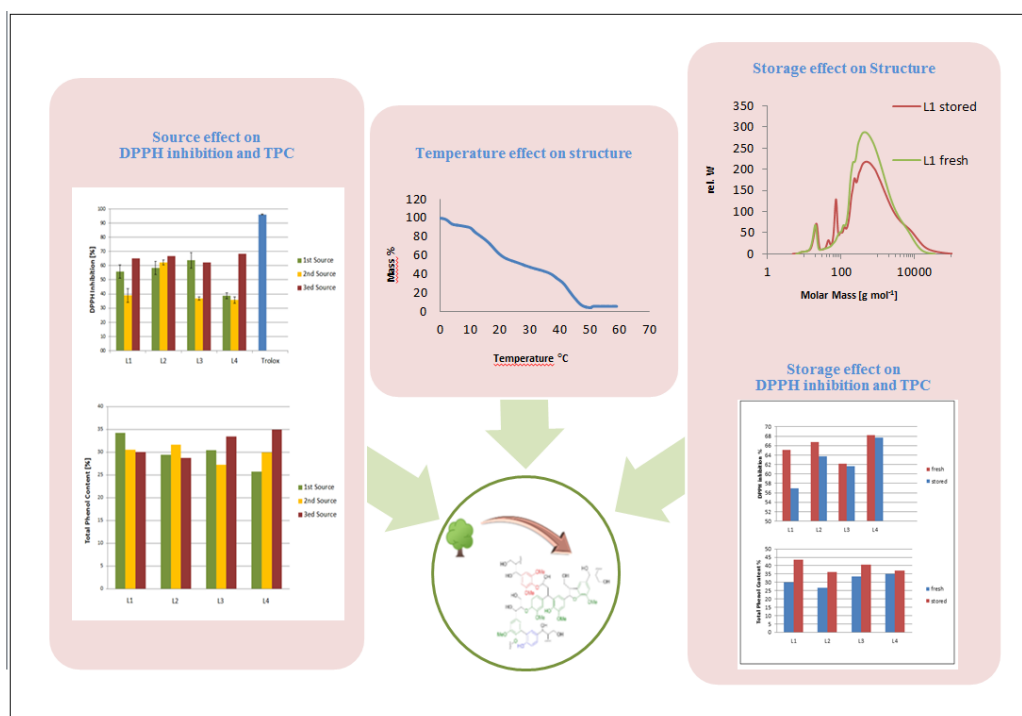
<sup>3</sup> Affiliation 3; Department of Forest Biomaterials, North Carolina State University, 2820 Faucette Drive Biltmore Hall, Raleigh, NC, USA 27695; [mclarki2@ncsu.edu](mailto:mclarki2@ncsu.edu) (M.L.)

<sup>4</sup> Affiliation 4; Kompetenzzentrum Holz GmbH, Altenberger Strasse 69, A- 4040 Linz, Austria; [b.kamm@kplus-wood.at](mailto:b.kamm@kplus-wood.at)

\* Correspondence: [margit.schulze@h-brs.de](mailto:margit.schulze@h-brs.de); Tel.: +49-2241-865-566; Fax: +49-2241-865-8566

**Abstract:** Antioxidant activity is an essential feature required for oxygen-sensitive merchandise and goods, such as food and corresponding packaging as well as materials used in cosmetics and biomedicine. For example, vanillin, one of the most prominent antioxidants, is fabricated from lignin, the second most abundant natural polymer in the world. Antioxidant potential is primarily related to the termination of oxidation propagation reactions through hydrogen transfer. The application of technical lignin as a natural antioxidant has not yet been implemented in the industrial sector, mainly due to the complex heterogeneous structure and polydispersity of lignin. Thus, current research focuses on various isolation and purification strategies to improve the compatibility of lignin material with substrates and enhancing its stabilizing effect.

This contribution presents antioxidant capacity studies of various lignins depending on purification degree of the raw material. In detail, the antioxidant potential of lignin-based compounds is studied using the DPPH (2,2-diphenyl-1-picrylhydrazyl) assay. The purification procedure was monitored by thin layer chromatography (TLC) and showed that double-fold selective extraction is the most efficient purification procedure (confirmed by UV-Vis, FTIR, HSQC and <sup>31</sup>P NMR spectroscopy, SEC and XRD analysis). Results are discussed regarding the dependency of antioxidant activity on lignin structure and biomass source. Thus, lignins obtained from industrial black liquor are compared with beech wood samples. In addition, the influence of lignin isolation (kraft *versus* organosolv) is discussed. Values of the antioxidant activity (DPPH inhibition) of kraft lignin fractions were 62–68% while beech and spruce/pine-mixed lignins showed values between 26, 64 and 42%, respectively. TPC values of the different isolated kraft lignin fractions varied between 26–35%, while beech, spruce/pine lignins were 34, 30 and 34%, respectively. Storage decreased the TPC values and increased the DPPH inhibition.



**Graphical Abstract.** Lignin antioxidant activity is studied regarding the influence of biomass source (soft and hard wood), pulping process (kraft *versus* organosolv), temperature and storage.

**Keywords:** antioxidant activity, biomass, Folin-Ciocalteu assay, lignin, lignocellulose feedstock, organosolv, total phenol content

## 1. Introduction

### 1.1 Lignin Availability and Structure

The main components of lignocellulosic feedstock (LCF) are cellulose, hemicellulose, and lignin (Figure 1). Lignin, a multi-substituted phenolic polymer, forms 15–30 wt% of dry LCF, accounting for up to 30% of the organic carbon on Earth. Roughly ten years ago, the first biorefinery concepts were reported [1,2]. Within the last decade, lignin has been intensively studied as one of the biorefinery platforms that can be used for aromatic chemical production and energy supplement [3–5].

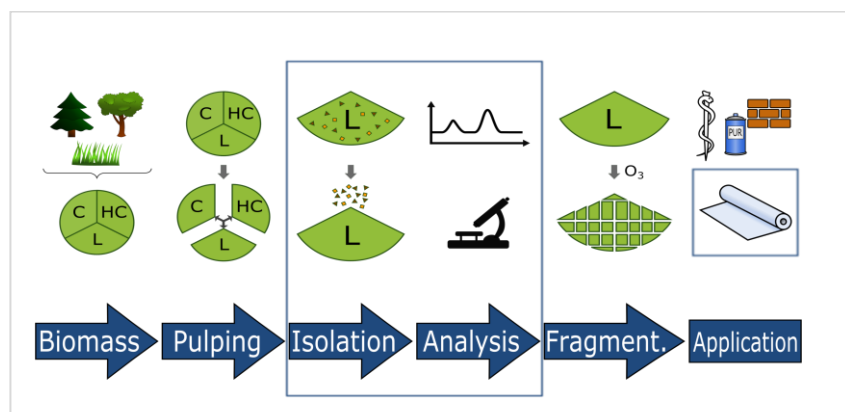


**Figure 1.** Development of lignin-derived materials starting with biomass pulping, lignin isolation and structure elucidation, guided fragmentation (e.g. ozonolysis), and application in construction, packaging and biomedicine (C: cellulose, HC: hemicellulose, L: lignin).

The main function of lignin is to give strength and mechanical support to the plant [6]. It is partially interconnected and forms a tight structure resistant to the influences of solvents and heat. Therefore, biorefinery concepts require efficient fractionation of the lingo-carbohydrate complex. Several methods to remove lignin from the biomass were developed including sulfate (kraft) and sulfite pulping [7], organosolv [8], alkaline polyol [9] and several steam explosion processes [10].

The biosynthetic precursors are comprised of three phenylpropanoid units (coniferyl, sinapyl, and *p*-coumaryl alcohol) that by various oxidative coupling reactions form a randomly cross-linked macromolecule with different inter-unitary linkages. The structural building blocks are joined together by ether linkages and carbon-carbon bonds, and consistent with the close association between lignin and hemicelluloses in the wood cell wall, there are also chemical bonds between these constituents [11].

The removal of lignin by kraft delignification is achieved by treating wood material in an aqueous solution of sodium hydroxide and sodium sulfide. Kraft lignin has several characteristic properties that distinguishes it from native and other technical lignins: kraft lignin contains a greater number of phenolic groups, due to the extensive cleavage of  $\beta$ -aryl bonds during kraft pulping, some biphenyl units, and other condensed structures as a result of the severe cooking conditions, see Figure 2 [12].

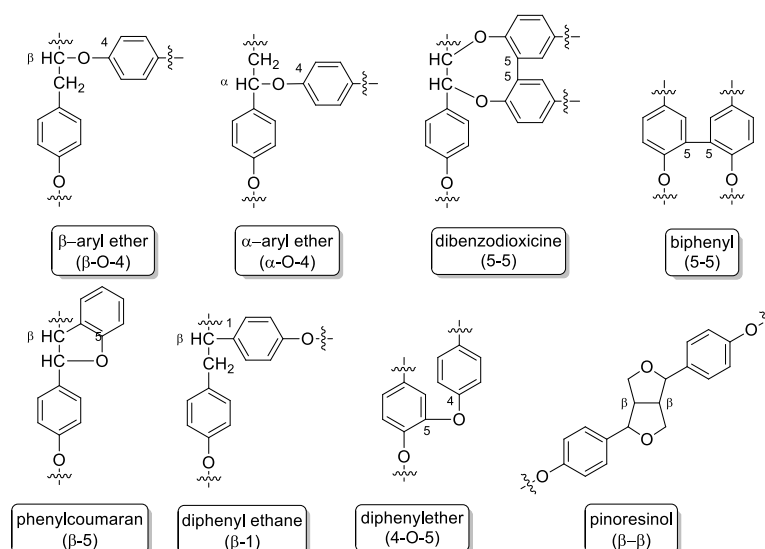


**Figure 2.** Lignin linkages: ether bonds, carbon-carbon bonds, and further more complex linkages.

Due to the low selectivity of kraft pulping, black liquor from this process still contains a significant amount of carbohydrate-derived substances, mainly aliphatic carboxylic acids [13,14]. Today, lignin as a source of phenolic units is one of the most lucrative candidates for various applications, e.g. as an emulsifier, adsorbent, carbon fiber precursor, antioxidant and co-reagent in phenol-formaldehyde resins and thermoplastics [15,16]. However, lignin valorization is still challenging due to its randomly-linked monolignol units resulting in a very complex and irregular chemical structure. Thus, improving lignin-derived materials for use in industrial applications is still limited to very few examples. The reproducible quality of the isolated structures requires much effort. Today, sequential depolymerization *via* oxidative or reductive methods is one of the favored approaches to generate well-defined lignin fragments, comprehensively reviewed by Schutyser *et al.* [17]. However, any additional chemical treatment comes with increased costs.

### 1.2 Antioxidant Capacity and Corresponding Assays

As a polyphenol, lignin has a strong potential as an antioxidant to prevent oxidation reactions in biofuels, animal feeds and polymeric composite materials. The complex structure of lignin,

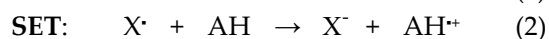
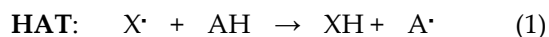
composed of aromatic rings with hydroxy and methoxy functional groups, is responsible for this antioxidant potential due primarily to the termination of the oxidation propagation reaction through hydrogen donation and single electron transfer reactions. The application of technical lignins as natural antioxidants has not been implemented in the industrial sector mainly due to the highly non-homogenous, complex structure and high polydispersity of lignin. Typically, purification and fractionation steps are necessary to enhance its stabilizing effect [18].

To determine the strength of an antioxidant, its ability to scavenge radicals or its reducing power is measured quantitatively. Several assays to determine the antioxidant capacity are reported for vanillin and corresponding derivatives in Garrett *et al.* [19]. However, reviewing the published studies on the antioxidant activity of vanillin Tai *et al.* concluded, that they are not consistent between assays. Thus, they systematically evaluated the antioxidant activity of vanillin using multiple assay systems (DPPH, ABTS and ORAC). Vanillin showed stronger activity than did ascorbic acid and Trolox in the ABTS•+- scavenging assay but showed no activity in the DPPH radical- and galvinoxyl radical-scavenging assays. Furthermore, vanillin showed much stronger activity than ascorbic acid and Trolox in the ORAC assay. In ABTS and ORAC assays, vanillin reacts with radicals via self-dimerization contributing to the high reaction stoichiometry against ABTS•+ and AAPH-derived radicals [20]. The most important assays used for lignin studies are shortly presented in Table 1.

**Table 1.** Antioxidant assays, the corresponding reaction mechanism, advantages and disadvantages.

| Antioxidant Assay  | Mechanism                | Advantages  | Disadvantages   | References |
|--|--------------------------|---|---|------------|
| ORAC (Oxygen Radical Absorbance Capacity)                      | Hydrogen Atom Transfer   | <ul style="list-style-type: none"> <li>• can be adapted to detect both hydrophilic and hydrophobic antioxidants by altering the radical source and solvent</li> <li>• ORAC values account for lag-time, initial rate and total extent of inhibition in a single value</li> <li>• automation is possible</li> </ul>  | <ul style="list-style-type: none"> <li>• to achieve reproducible results, reaction conditions (temperature, pH, oxygen and reagent concentrations etc.) have to be observed critically</li> <li>• detection requires fluorometer (fluorescence easy to be quenched)</li> <li>• analysis time about one hour</li> <li>• measurement is limited to peroxy-radicals as oxidants</li> </ul> | [19]       |
| FRAP (Ferric Reducing Antioxidant Power)                       | Single Electron Transfer | <ul style="list-style-type: none"> <li>• simple, quick, inexpensive, robust, does not require special equipment</li> <li>• direct method to measure the combined activity of multiple, reductive antioxidants in a sample</li> <li>• automation is possible</li> </ul>  | <ul style="list-style-type: none"> <li>• no exact reaction time / reactivity is varying for different samples</li> <li>• thiol-containing antioxidants like glutathione are not detected</li> </ul>   | [20]       |
| CUPRAC (Cupric Reduction Antioxidant Capacity)                 | Single Electron Transfer | <ul style="list-style-type: none"> <li>• simple, quick, inexpensive, robust, does not require special equipment</li> <li>• all classes of antioxidants are detected, including thiols</li> <li>• applicable to both, hydrophilic and lipophilic antioxidants</li> </ul>   | <ul style="list-style-type: none"> <li>• no exact reaction time / reactivity is strongly varying for different samples</li> </ul>   | [21]       |
| ABTS (2,2'-azino-bis(3-ethylbenzothiazoline-6-sulphonic acid)) | mixture of HAT / SET     | <ul style="list-style-type: none"> <li>• simple, quick, wide pH-range, often used</li> <li>• soluble in aqueous and organic solvents and not affected by ionic strength -&gt; applicable to a wide range of hydrophilic and lipophilic antioxidants</li> <li>• several wavelengths are available for photometric detection of the ABTS-radical</li> </ul> | <ul style="list-style-type: none"> <li>• no exact reaction time / reactivity is strongly varying for different samples</li> <li>• the bulky ABTS-radical is not a good model for small, biologically more relevant radicals like HO• etc.</li> </ul>  | [22]       |
| DPPH (2,2-diphenyl-1-picrylhydrazyl)                           | mixture of HAT / SET     | <ul style="list-style-type: none"> <li>• simple, quick, often used, no special equipment needed</li> <li>• DPPH-radical is commercially available; no <i>in situ</i> - generation necessary</li> </ul>  | <ul style="list-style-type: none"> <li>• no exact reaction time / reactivity is varying for different samples</li> <li>• DPPH-radical may have a poor reactivity with antioxidants due to its stability and sterical hindrance</li> </ul>   | [23]       |
| FC/TPC (Folin-Ciocalteu-Assay or Total-Phenolics-Assay)        | mixture of HAT / SET     | <ul style="list-style-type: none"> <li>• simple, often used, does not require special equipment</li> </ul>  | <ul style="list-style-type: none"> <li>• no exact reaction time / reactivity is varying for different samples</li> <li>• interferences with other reductive substances may influence the results</li> </ul>   | [24]       |

Basically, assays can be divided in two mechanisms: the *Hydrogen Atom Transfer (HAT)* mechanism; here, radicals are quenched by hydrogen atom donation of the antioxidant, while in the *Single Electron Transfer (SET)* mechanism, the antioxidant's ability to transfer one electron to reduce any compound is used (Equations 1 and 2).



where  $X^\bullet$  is the radical, AH the antioxidant, resulting in protonated radical XH and antioxidant radical, or anion  $X^-$  and radical cation  $\text{AH}^{+\bullet}$ .

Often, both mechanisms occur in parallel resulting in very complex reaction kinetics and numerous side reactions. Most relevant criteria for determining the mechanism and the efficacy of antioxidants are their bond dissociation energy and ionization potential. In fact, polyphenols, as lignins, possess multiple activities. Thus, their antioxidant activity depends on the medium and corresponding solubility as well as testing substrate.

The *Oxygen Radical Absorbance Capacity* (ORAC) assay is based on the interaction of the peroxy-radical  $\text{ROO}^\bullet$  with fluorescein. ORAC values are usually reported as Trolox equivalents with help of a standard curve for measurements of Trolox samples of different concentrations [21]. Ponomarenko *et al.* studied the fractionation of soft and hardwood LignoBoost kraft lignins, using sequential extraction with organic solvents, and reported that all fractions showed good results in the ORAC assay at the level of Trolox or even better [22]. In the *Ferric Reducing Antioxidant Power* (FRAP) assay, reduction of ferric 2,4,6-tripyridyl-*s*-triazine (TPTZ) to a colored product is measured photometrically [ $\text{Fe(III)}/\text{Fe(II)}$ ] [23]. Antioxidant compounds with a redox potential below 0.7 V can be detected. The *Cupric Reduction Antioxidant Capacity* (CUPRAC) assay is a variant of the FRAP assay, using a [ $\text{Cu(II)}/\text{Cu(I)}$ ] reduction which makes this assay more selective than the FRAP assay due to the lower redox potential [24]. So, sugars (potential residuals of biomass pulping) are not detected by this assay. The ABTS (2,2'-azino-bis(3-ethylbenzo thiazoline-6-sulphonic acid) assay is also based on a redox reaction of the ABTS radical cation. Results are expressed relative to Trolox [25]. Analogously, the DPPH assay uses the redox reaction of the 2,2-diphenyl-1-picrylhydrazyl or DPPH with an antioxidant resulting in reduced color intensity proportional to the antioxidant concentration [26]. The *Folin Ciocalteu Assay* or *Total Phenolics Assay* has been used to measure the total phenol content (TPC) of natural products for many years. The Folin-Ciocalteu reagent (a mixture of phosphomolybdate and phosphotungstate) reacts with an antioxidant, thereby changing the color intensity proportionally to the antioxidant concentration. Gallic acid is used as a reference compound and results are expressed as *Gallic Acid Equivalents* or TPC [27].

Comparing these assays, it is most important to identify the type of radicals is most crucial for *in vivo* conditions, i.e. using lignin as antioxidative additive in food, cosmetics or biomedicine [28, 29]. Here, the ORAC-Assay is of advantage since peroxy radicals  $\text{ROO}^\bullet$  are more related to *in vivo* conditions than  $\text{DPPH}^\bullet$ - and  $\text{ABTS}^\bullet$  radicals due to their size. Thus, steric hindrance of  $\text{DPPH}^\bullet$ - and  $\text{ABTS}^\bullet$  radicals influence the reaction kinetics [25]. In addition, results of the ORAC assay are independent of the reactivity rate in the antioxidant/substrate system. Contrary to this, the evaluation of FRAP, CUPRAC, ABTS and DPPH assays need chosen reaction end points. However, these end-points usually do not represent the exact potential of the antioxidant.

So far, the antioxidant activity of lignin samples is mainly studied using the DPPH assay and Folin-Ciocalteu method. Telysheva *et al.* developed structure-property relationships regarding antioxidant activity proposing that the  $\pi$ -conjugation systems of lignins operate as catalysts/activators in the interaction with DPPH radicals while heterogeneity and polydispersity decrease the antioxidant efficiency critically. Using EPR spectroscopy to characterize paramagnetic polyconjugated clusters in lignin samples, it was confirmed that paramagnetic polyconjugated clusters resulted in a linear increase in antioxidant capacity whereas aromatic OH and  $\text{OCH}_3$  contents are of lower influence [29]. Santos *et al.* studied isolation and purification effects including solvent influence comparing water and organic solvents versus alkaline solution. They found that lignins with a low percentage of phenols showed the highest elimination of DPPH radicals [30].

Aminzadeh *et al.* used membrane filtration for LignoBoost kraft lignin fractionation (molecular weight cut-off of 1 kDa) to evaluate antioxidant activity using the ORAC assay. According to 2D NMR, membrane filtration resulted in lignin oligomers with a high content of methoxy groups; 31P

NMR spectroscopy showed a higher proportion of non-condensed phenolic OH groups for samples of lower TPC. ORAC tests of low MW fractions showed higher antioxidant activity than the non-fractionated LignoBoost and three-fold stronger inhibition of the substrate (fluorescein) than Trolox [31].

2. Results and Discussion

2.1. Lignin Structure Analysis

Structural analysis to specify accessible functional groups is essential to classify lignins for further studies regarding antioxidant capacity and related structure-property relationship [5, 32, 33]. Kraft lignin functional groups obtained in this study are listed in comparison with literature data in Table 2. Thus, all four fractions contain the main and essential functional groups identifying lignin as reported in literature [34, 35]. L4 has the broadest OH stretching peak due to it having the least impurities. The broadness of this peak decreases when going in a reverse order (i.e. from L4 to L1). The spectra also show fewer impurities as well less noise: signal ratio going from L1 to L4 confirming the purification procedure.

Table 2. FTIR functional group assignment of lignin fractions.

| L1                  | L2                  | L3                  | L4                  | KL lit. [34, 35]    | signal assignment  |
|---------------------|---------------------|---------------------|---------------------|---------------------|--|
| [cm <sup>-1</sup> ] | [cm <sup>-1</sup> ] | [cm <sup>-1</sup> ] | [cm <sup>-1</sup> ] | [cm <sup>-1</sup> ] |  |
| 3396                | 3408                | 3414                | 3396                | 3415                | O-H stretching   |
| 2931                | 2931                | 2926                | 2925                | 2935                | C-H stretching   |
| 2834                | 2814                | 2834                | 2833                | 2843                | tertiary C-H group                                       |
| 1695                | 1695                | 1700                | 1702                | 1660                | carbonyl-carboxyl stretching                             |
| 1577                | 1583                | 1593                | 1595                | 1505                | aromatic/carbonyl stretching                             |
| 1452                | 1449                | 1455                | 1459                | 1451                | C-H deformation  |
| 1263                | 1262                | 1265                | 1262                | 1265                | C-O stretching, aromatic (phenyl)                        |
| 1028                | 1028                | 1026                | 1028                | 1029                | C-O deformation (methoxy group)                          |
| 810                 | 810                 | 807                 | 807                 | 814                 | C-H out-of-plane in <i>m</i> -position of guaiacyl units |
| 848                 | 848                 | 848                 | 848                 | -                   | C-H out-of-plane in <i>m</i> -position of guaiacyl units |

UV/Vis studies (Fig. 3) clearly show the difference between the lignin fractions. Significant improvement could be achieved. Thus, L4 shows four distinct UV peaks (no shoulders any longer) due to  $\pi-\pi^*$  and  $n-\pi^*$  excitations of conjugated phenolic groups, while in literature most of the spectra of kraft lignin contain at least two shoulders as shown for the first three fractions L1 to L3 of the purification procedure [34]. Due to the hypsochromic effect of NaOH the main absorption (usually around 280 nm) is shifted to 214-222 nm.

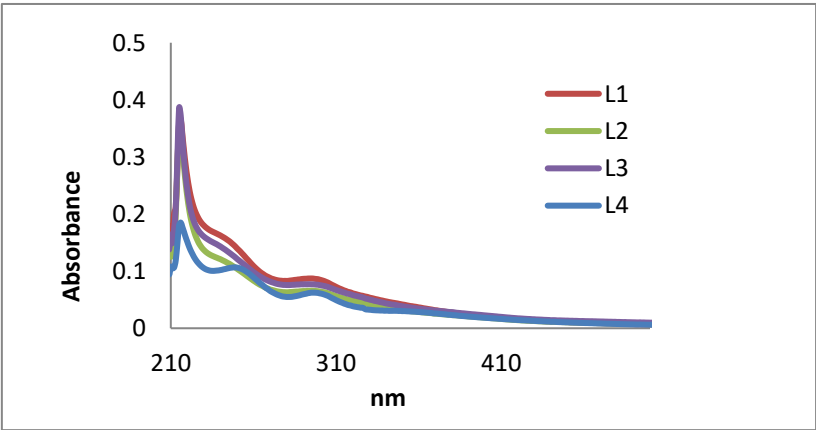




**Figure 3.** UV/Vis analysis of kraft lignin purification fractions (solved in NaOH): L1 (red), L2 (green), L3 (purple) and L4 (blue).

In Table 3, the two main UV/Vis absorption bands of lignin are shown and compared with literature data. Accordingly, the ester or ether bonds between acids, ferulic acids and lignin were substantially cleaved by the alkali treatment. The intensive absorbance at 279–280 nm relatively to 316–320 nm indicates a high content of guaiacyl (G) units, similar to that of other monocotyledons and is consistent with a guaiacyl-rich lignin [35,36].

**Table 3.** UV-Vis absorption data of lignin and their characteristics.

| $\lambda$ exp. [nm] | $\lambda$ lit. [nm] | Functional group  | Intensity | Excitation    | Reference                     |
|---------------------|---------------------|---|-----------|---------------|-------------------------------|
| 215–222             | 279–280             | Non-conjugated phenolic groups (G/S rich)                           | high      | $\pi - \pi^*$ | Azadi <i>et al.</i> [36]      |
| 296–303             | 316–320             | Conjugated phenolic groups ( <i>p</i> -coumaric acid, ferulic acid) | low       | $n - \pi^*$   | Vivekanand <i>et al.</i> [35] |

Three regions of lignin structure can be identified via 2D HSQC NMR (Fig. 4): non-oxygenated and oxygenated aliphatic side chains appear at  $\delta C/\delta H$  50.0–90.0/2.5–6.0, and the aromatic region with C-H correlation signals at  $\delta C/\delta H$  100.0–135.0/5.5–8.5 confirming literature data [12]. The following spectra exhibit intense signals at 56/3.7 corresponding to methoxyl groups and side chains in  $\beta$ -O-4-structures. Furthermore, a signal at 62/3.2 attributed to the gamma-C-H of gamma-acylated lignin units. A prominent region is located at 110–120/ 6.4–7 correlating with C-H aromatic signals from G units, while signals higher than 120 relate to aromatic C-H signals from H units.

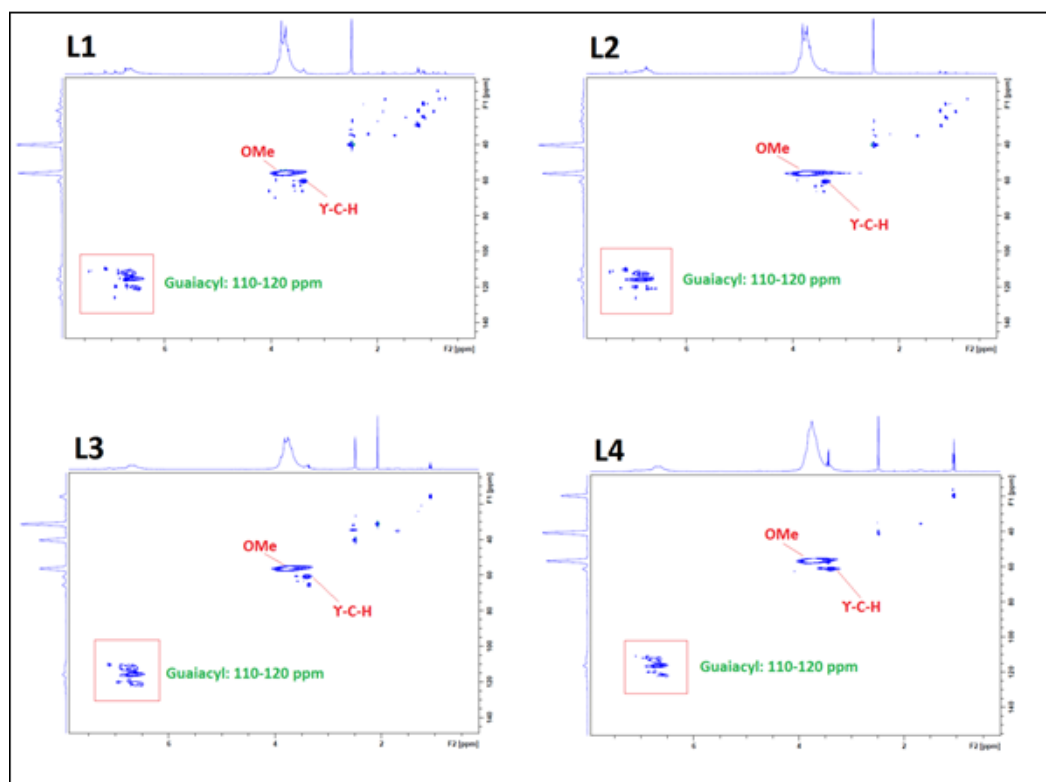


**Figure 4.** HSQC NMR spectra of kraft lignin purification fractions L1, L2, L3 and L4; specifying in particular OMe signals, Y-C-H signals, G-unit signals.

To analyze lignin more in detail, phosphorous derivatization is an appropriate and widely accepted method [37]. However, the sensitivity of a  $^{31}\text{P}$  NMR experiment is about 15 times less than that of a proton NMR experiment, and the range of  $^{31}\text{P}$  chemical shifts is more than 1,000 ppm for a variety of phosphorous compounds. The  $^{31}\text{P}$  NMR spectra in Fig. 8 show five OH regions for the lignin fractions: aliphatic OH between 151.0–144.7, 5-substituted OH between 144.0–142.3, guaiacyl OH between 142.5–141.5, *p*-hydroxyphenyl between 141.5–141.1, and carboxylic acids between 141.1–135.9. All lignin samples were phosphorylated with 2-chloro-4,4,5,5-tetramethyl-1,2,3-dioxaphospholane and analyzed via quantitative  $^{31}\text{P}$  NMR spectroscopy (with endo-N-hydroxy-5-norbornene-2,3-dicarboximide as internal standard) according to the method described by Sun *et al.* [38]. As shown in Fig. 5, aliphatic OH's are dominant except for L3 where COOH OH's are more intense. In L1, the ratio of COOH-OH to aliphatic OH is almost 1:1, while aromatic OH form almost half of the aliphatic OH indicating the presence of some small fragments or carbohydrates in L1. In L2, the aliphatic OH number is 11 times higher than the COOH. Most probably, carboxylic acid containing fragments were dissolved by the diethylether during extraction and discarded with the filtrate with some of the aliphatic OH containing fragments. Extracting the lignin from L1 using acetone led to the loss of some aliphatic OH-containing compounds and the number of the aliphatic OH dropped almost to the half. Those fragments possibly are small fragments that could be dissolved with acetone and discarded with the filtrate. In L4, where ethanol is used for the selective extraction of L3, the number of the COOH-OH's dropped by the half and the number of aromatic OH's dropped around five-fold. The number of the aliphatic OH groups did not change significantly. Those results coupled with further analytical data (i.e. FTIR, UV/Vis, SEC, DSC, TGA) prove the effect of the purification procedure.

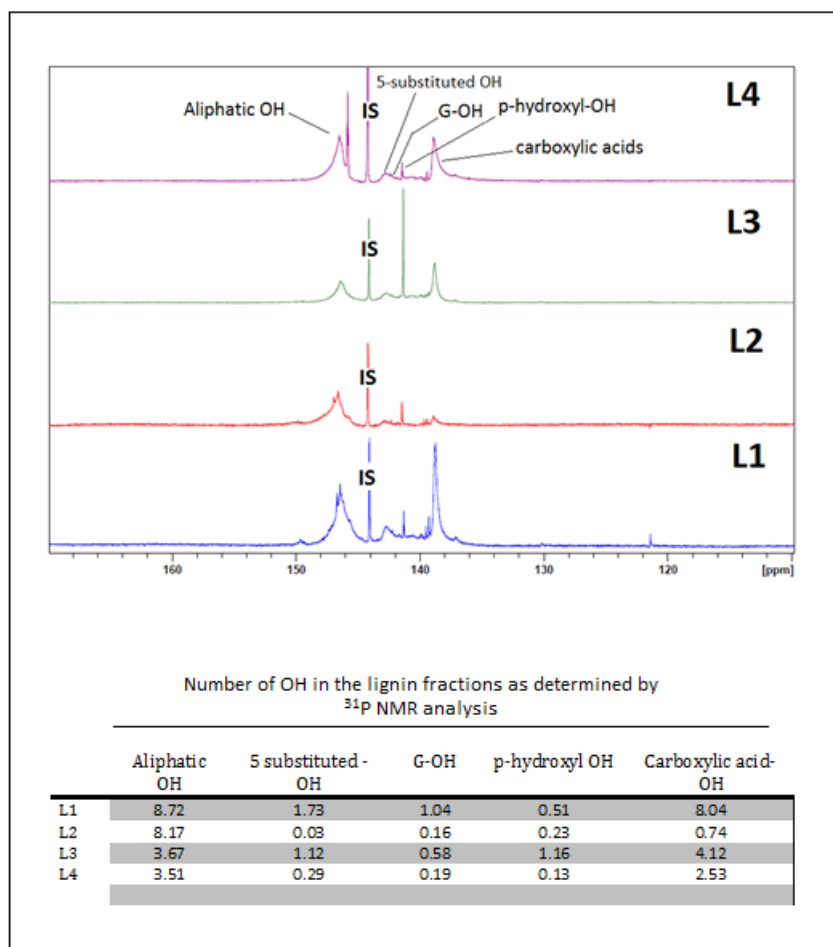


**Figure 5.**  $^{31}\text{P}$ -NMR spectra of kraft lignin purification fractions: L1, L2, L3 and L4. The table shows the corresponding OH number in the fractions.



The molar mass distribution is a key analytical parameter for technical lignins. Various approaches are reported on how to address the molar mass distributions of lignins mainly using size exclusion chromatography (SEC), viscosimetry, and light scattering analyses [39]. The main drawback of SEC studies is the utilization of polymethylmethacrylate (PMMA) or polystyrene (PS) standards due to the lack of appropriate lignin standards. Both PMMA and PS do not represent the hydrodynamic volume of lignin. However, universal calibration approaches would require precise concentration data which are also difficult to determine due to the poor solubility of lignin. A novel approach using SEC and HSQC NMR data combined with multivariate data analysis enables access to molecular weight and polydispersity data was recently reported for heparin [40]. In our studies, using PMMA, the molecular weight of the isolated fractions varies from 877 to 6117 g mol<sup>-1</sup> which corresponds to literature values for comparable technical lignins [12, 30]. Figure 6 shows the SEC results of the four kraft lignin fractions (L1 to L4) and the corresponding data (Mw, Mn and PD).

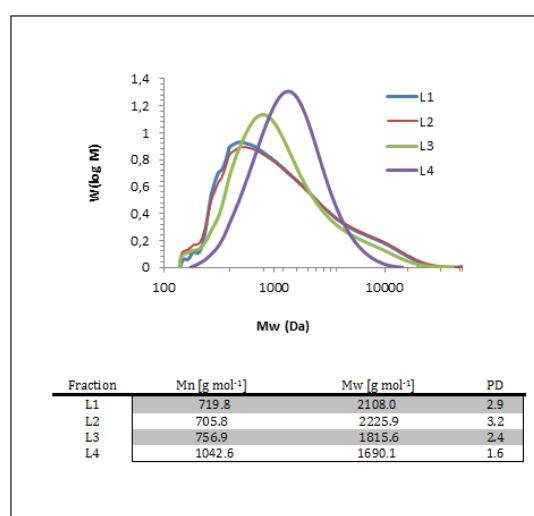


**Figure 6.** SEC analysis of kraft lignin purification fractions: L1 (blue), L2 (red), L3 (green) and L4 (purple), molecular weights (Mn, Mw) and polydispersity (PD) values.

For all fractions, there is a clear dependency between purification and resulting SEC data. In L4, the spectrum shows one peak with a maximum of 1157 g mol<sup>-1</sup>. The curves of L1, L2 and L3 have more than one peak with low molecular weights, representing smaller fragments and/or impurities. The maxima's of L1, L2 and L3 are 484, 466 and 878, respectively, with increasing intensity as the number of impurities or smaller fragments decreases.

Lignin, being a three-dimensional amorphous polymer connected by phenylpropane structural units through  $\beta$ -O-4 ether and C-C linkages, contains a variety of reactive functional groups, in which methoxy is the most prominent group. According to the differences in the side chains, various structural fragments can be formed: guaiac wood-based lignin, lilac lignin, and hydroxyphenyl lignin, which can result in the formation of various phenolic compounds such as 2-methoxyphenol, 4-methylguaiacol, 2-methoxy-4-nylphenol, through propylene side chain splitting. The cleavage of the C-C bond in the guaiac wood-based lignin will generate vanillin, while other products, such as ethers, alcohols, etc. may be formed by unstable fracture of long straight side chain in complex macromolecular structure of lignin.

Although lignin only has three basic structural units, the reactivity of the functional groups at the aromatic rings of each basic structural unit is different. This results in a high complexity in the pyrolysis process of lignin [41]. Figure 7 shows the Py-GC/MS chromatograms for the fractions L1, L2, L3 and L4 with the assignment of the main signals.

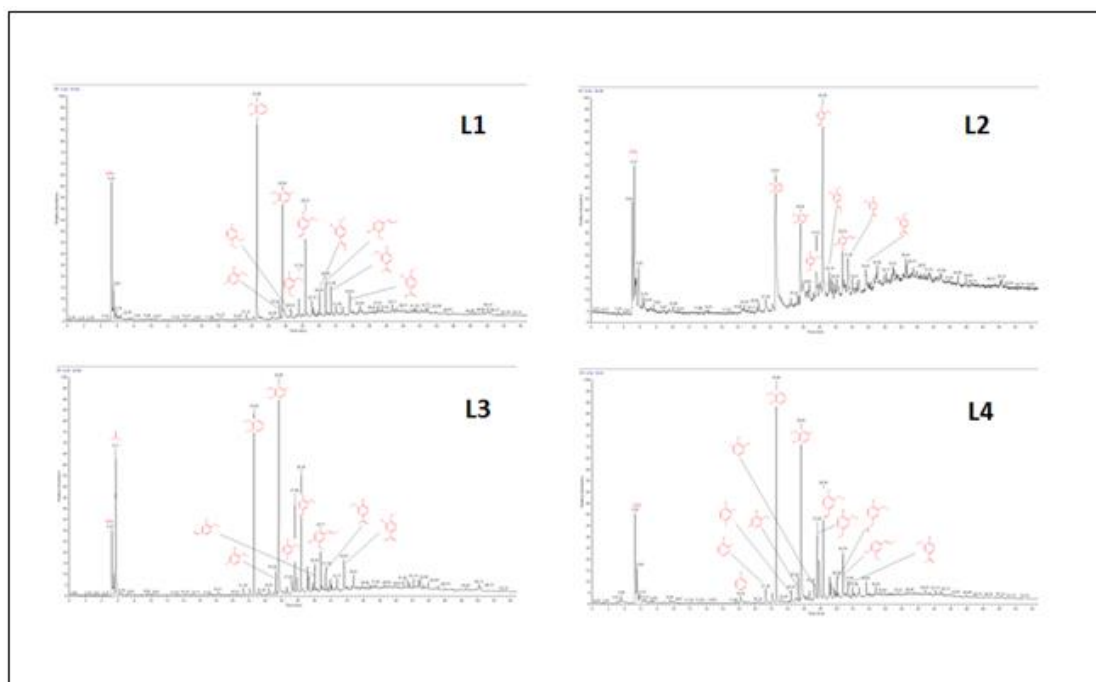


**Figure 7.** Pyrograms of kraft lignin purification fractions: L1, L2, L3 and L4 (measured at 550 °C).

Thermogravimetric analysis (TGA) is used to determine the mass loss of samples due to the temperature treatment, as indicative of thermal stability and thermal decomposition of a compound. Here, TGA of the lignin fractions was measured according to a procedure used by Vallejos *et al.* (Figure 8) [42]. The L1 TGA curve shows a complex decomposition process that resulted from five overlapping steps with the main maximum of mass loss rate at 60, 240, 380, 790 and 880 °C. The total mass loss is 82.08 wt%. L2 decomposes in four steps at 60, 372, 780 and 880 °C. The total mass loss is 76.90 wt%. The decomposition in L3 occurs by four steps: 60, 150, 395 and 900 °C. The total mass loss is 99.79 wt%. L4 decomposes at 60, 377, 810 and 900 °C. The total mass loss is 99.91%. In the TLC spotting of the lignin fractions occurs at 25, 40, 60 and 90 °C; a new spot appearing for the fractions at 60 and 90 °C likely can be assigned to a fragment in the mobile phase, not necessarily evaporating water.

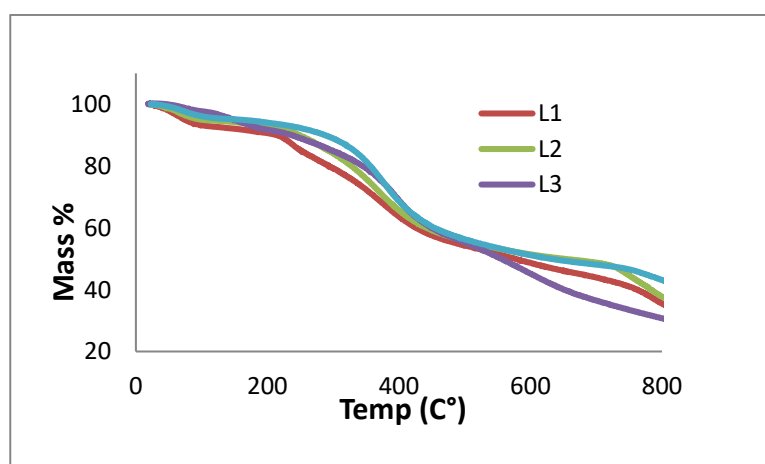


**Figure 8.** TGA curves for kraft lignin purification fractions: L1 (red), L2 (green), L3 (purple) and L4 (blue) (measured from 0 to 800 °C).

The first weight decrease (up to 259 °C) is ascribed to the moisture content in the lignin and the release of volatile products such as carbon monoxide and carbon dioxide. Additionally, creation of vinyl guaiacol, ethyl, and methyl by-products is usually observed between 230 and 260 °C with the

degradation of propanoid side chains of lignin [32, 33]. In the temperature range of 160–270 °C, it is also seen that thermal treatment of lignin was followed by condensation processes and led to the formation of unsaturated C=C bonds. The major decomposition of lignin structure occurred in the range 260–478 °C. At temperatures lower than 310 °C, cleavage of aryl ether links occurs due to its low thermal stability. Eventually, the final stage happened after 478 °C which involved in formation of char residues [43].

Lignin is an amorphous polymer that undergoes changes in physical characteristics upon heating, resulting in transitions to a glassy and rubbery state. The glass transition temperature ( $T_g$ ) of lignin is affected by factors such as presence of low molecular weight contaminants (including water and solvents), molecular weight, thermal history, crosslinking, etc. [12, 43]. DSC measurements show that the  $T_g$  of L4 has the highest value of 185.15 °C, 140.15 °C for L2, 125.72 °C for L3 and 123.32 °C for L1. In accordance to literature data, these  $T_g$  values are associated to hydrogen bonds between hydroxyl groups and to the lignin aromatic nature (Figure 9) [44].

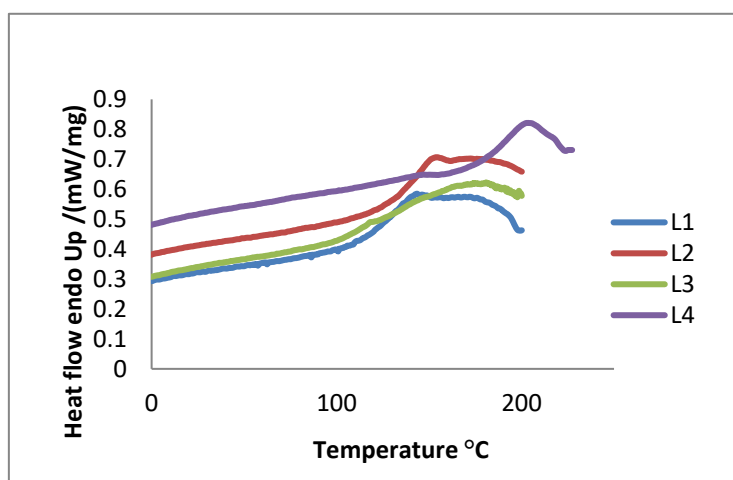


**Figure 9.** DSC curves of the kraft lignin purification fractions L1 (blue), L2 (red), L3 (green) and L4 (purple).

X-ray diffraction studies were performed to study the lignin morphology more in detail. All lignin fractions showed a broad diffraction of amorphous halo with a maximum at about  $2\theta = 20^\circ$  (Fig. 10). In fractions L1, L2 and L3, there were some sharp peaks indicating a certain crystallinity due to impurities and/or small crystalline fragments (as discussed for the SEC results). L4 showed an amorphous pattern with no sharp peaks at all. The intensity increased with the purification level from L1 to L4. As the crystallite signal size is reduced, the diffraction peaks broaden. Once the size is sufficiently reduced, the crystalline diffraction peaks may have broadened to the extent that they merge into each other, forming a single broad diffraction peak (the blue halo) supporting the amorphous nature of lignin and proving the effect of the purification procedure (Fig. 10).

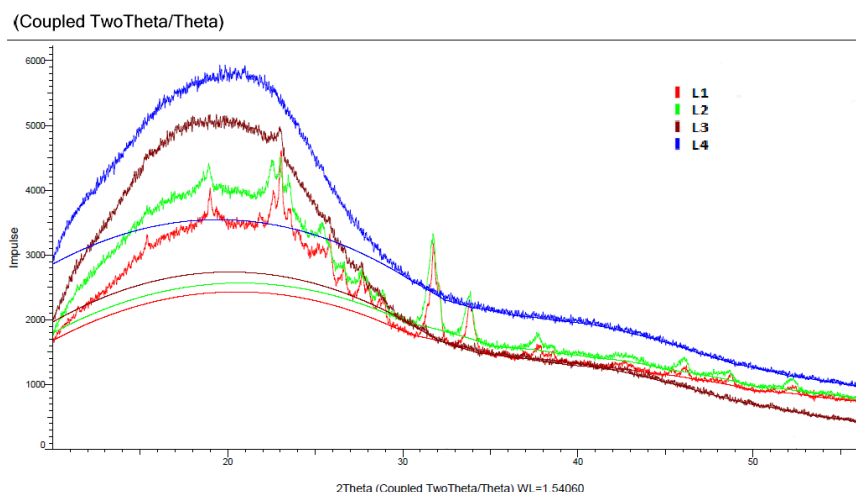


**Figure 10.** XRD diffractogram of the kraft lignin purification fractions L1 (red), L2 (green), L3 (brown) and L4 (blue).

## 2.2 Antioxidant Activity and TPC

The antioxidant activity of the lignin fractions was evaluated using the DPPH method according to studies reported by Santos *et al.* [23]. The reactivity of DPPH is far lower than that of oxygen containing free radicals (OH, RO, ROO and O<sub>2</sub>), and unlike them, the interaction rate is not diffusion-controlled. Rather good conformity of the results obtained by the DPPH and ABTS method, respectively, has been reported [4]. As their free radical scavenging ability is facilitated by their hydroxyl groups, the total phenolic content is used as a rapid screening of antioxidant activity (measured as chemical reducing capacity relative to gallic acid). Here, the TPC was determined using the Folin–Ciocalteu reagent. Table 4 shows the DPPH inhibitions of lignin fractions compared to organosolv lignin obtained from beech (DL) and organosolv lignin obtained from spruce and pine (OLSW).

**Table 4.** The DPPH inhibitions and TPC values of kraft lignin fractions (L1 to L4) and organosolv lignins obtained from beech (DL) and spruce/pine (OLSW).

|                          | L1       | L2       | L3       | L4       | DL       | OLSW     | Lit. [28] |
|--------------------------|----------|----------|----------|----------|----------|----------|-----------|
| <b>DPPH inhibition %</b> | 65.1±3.7 | 66.8±6.6 | 62.2±9.5 | 68.2±3.6 | 64±2.6   | 42±1.9   | 54.76     |
| <b>TPC %</b>             | 30±1.2   | 26.8±0.5 | 33.5±0.9 | 35±1.0   | 33.3±1.6 | 34.1±1.0 | 29.61     |

Values are mean ± standard deviation of triplicate experiments. Trolox DPPH inhibition % = 98 % [28].

All kraft lignin fractions exhibited higher DPPH inhibition compared to literature data of kraft lignin isolated under same conditions. L4 (extracted from ethanol) recorded the highest among them and L3 (extracted from acetone) the least. Variations in the antioxidant capacity of different fractions are mainly attributed to differences in their phenolic content and the type of phenolics which in turn depends on the solvent used for the extraction [45].

In this study, it is clear that the DPPH inhibition is affected by the polarity of the extraction solvent. Thus, the trend in DPPH inhibition of lignin fractions is ethanol > diethylether > acetone. Here there were two factors affecting the activity: first is the presence of fragments, and second the solvent polarity. In the first two fractions (L1 and L2), the number of impurities is higher than in L3 and L4; those impurities could include small molecular weight phenols (monomers) which exhibit a certain antioxidant activity. Second, the extraction solvent polarity significantly influences the amount of accessible phenolics responsible for the antioxidant activity.

TPC values of the kraft lignins studied are between 26.8–35%, while Santos *et al.* reported maxima of 29.61 % [30]. The TPC values show that purifying the lignin starting from L1 to L4

increased the phenolic content (except for L2 where diethyl ether was used to soak). For L4, the last extraction fraction of highest purity shows the highest TPC value. Obviously, the solvent used in the purification significantly affected the TPC data as reported for studies of polyphenol extraction from different plants, confirming a proportional effect of solvent polarity and TPC value [45, 46]. Here, we can confirm those results for the solvent extraction using ethanol, acetone and diethyl ether. Diethyl ether, being the least polar among them, has a negative effect on the TPC of the extracted lignin and ethanol, being the most polar, has a positive effect. Organosolv-derived lignins (OLSW and DL) possess a higher TPC compared to kraft lignins, indicating that the organosolv process keeps a reasonable amount of phenolic structure in the lignin. As reported in various literature studies, there is no clear correlation between DPPH inhibition and TPC values, most probably due to the type of phenolics responsible for the antioxidant activity [46].

### 2.2.1 Source, Storage and Temperature Effect

Three different batches of the black liquor were used for the extractions. The products of those extractions were grouped into three sets each that represent one source. The analytical characterization of those three sets of fractions show slight differences on the lignin structures. DPPH inhibition and TPC of the three sets were carried out (Fig. 11) and showed deviations without clear correlation or trend. This could be caused by differences in the harvesting time of the biomass, the age of the biomass used for the pulping and/or the percentage of the spruce/pine in the biomass pulped.

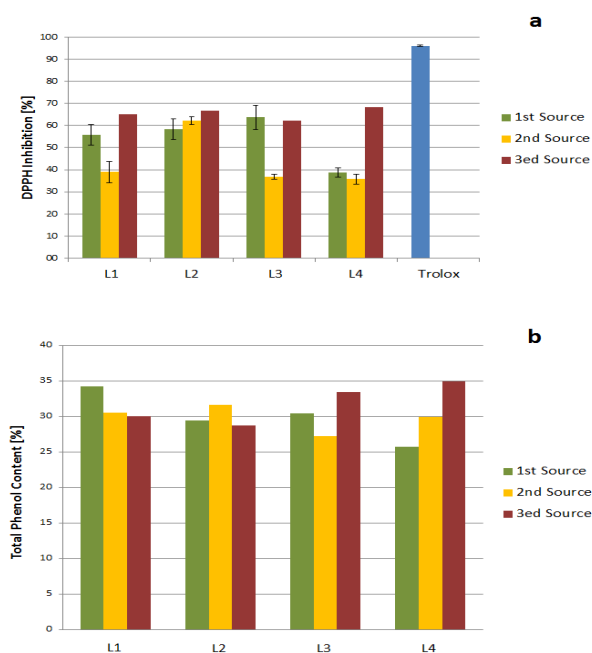


**Figure 11.** Source effect on **a)** DPPH inhibition and **b)** Total Phenol Content (1<sup>st</sup> source green, 2<sup>nd</sup> source yellow and 3<sup>rd</sup> source red).

Storage effect on the antioxidant activity and the TPC of the purification fractions was also investigated. The fractions were studied after purification then stored for 6 months. The DPPH inhibition and TPC were carried out again for the stored fractions. The results (Fig. 12) showed that the effect of storage on the DPPH inhibitions of the fractions decreasing for all fractions. In contrast, the TPC of the fractions increased, likely due to hydroxyl formation during storage. Obviously, none of them influenced the antioxidant activity. In ongoing studies, the structure of those degradation products will be analyzed.

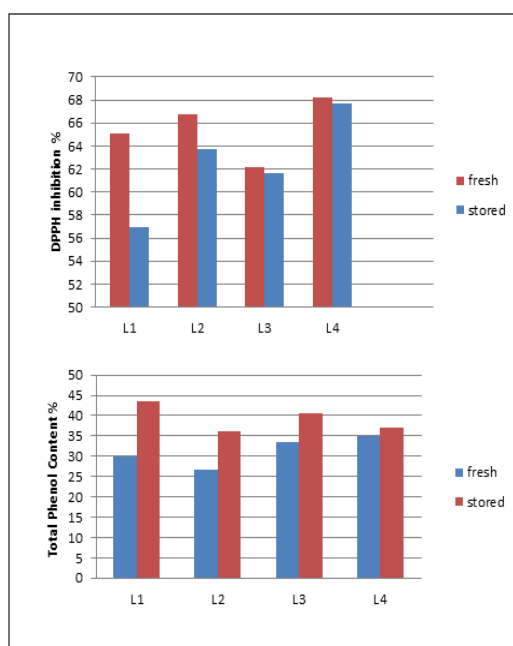


**Figure 12.** Above: Storage effect on DPPH inhibition of the kraft lignin purification fractions (fresh samples in red and stored in blue); Below: TPC (fresh samples in blue and stored in red).

Degradation processes of the macromolecular lignin structure were not only affected by storage, but also by temperature and UV/Vis irradiation. Thus, storing lignin purification fractions for 45 days at room temperature caused structural changes that were monitored by thin layer chromatography (TLC). The solvent system used for the study was 90 % ethanol and 10 % n-hexane. L1 showed three spots: one dense spot at the baseline which is the lignin spot, a second spot (small and light) located in the middle of the TLC sheet, and a third spot (large) traveling with the mobile phase. After 45 days of storage, TLC was repeated for the fractions showed that the spot in the middle for L1 looked denser and bigger than for fresh L1. This means that there were new fragment(s) in the lignin caused by degradation due to storage. SEC (GPC) analysis of both stored and fresh extracts showed this fragmentation clearly (Fig. 13a): new peaks at smaller molecular weights ( $45 \text{ g mol}^{-1}$  and  $73 \text{ g mol}^{-1}$ ) appear for the stored samples. The fragmentation was not caused by thermolysis since storage was performed at  $25^\circ\text{C}$ , nor by any chemical interaction. Samples were stored in aluminum foil-coated vials to prevent light from contributing to photolytic degradation, which in principle is observed and studied in detail for various lignins [47, 48].

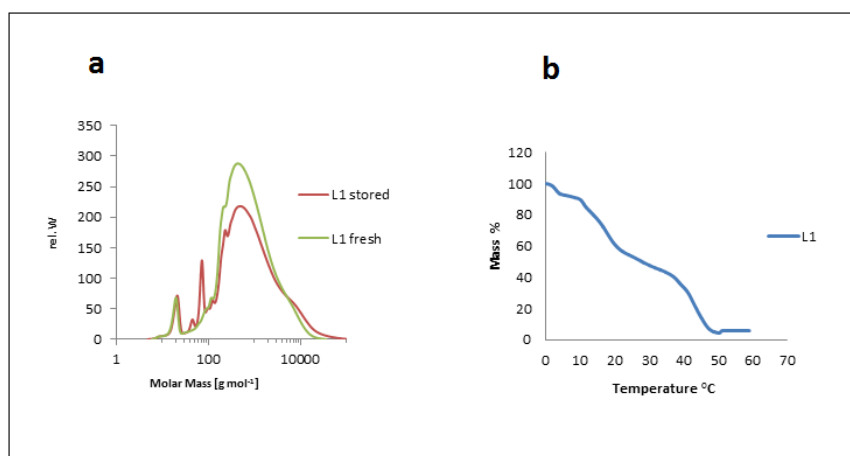


**Figure 13.** a) Storage effect on lignin structure via the SEC analysis of freshly isolated (green) versus stored (red) lignin (sample L1). b) Temperature effect on the structure of lignin via the TGA thermal analysis of Kraft lignin (sample L1).



The samples were dried at different temperatures: 25, 40, 60, 70, and 90 °C. TLC spotting showed no change in the L4 (one spot at 25 °C and 40 °C), but a new spot for L4 traveling with the solvent system appeared at 60, 70 and 90 °C in addition to the lignin spot. The second spot (in the middle of the TLC plate) of the L1 fraction became denser and bigger than that in the dried fraction at 25 °C and 40 °C. TGA was measured for the lignin fraction according to Vallejos *et al.* [42]. The curve of L1 shows the temperatures for lignin degradation were mainly: 60, 380, and 880 °C. The degradation temperatures for L4 were: 60, 390 and 900 °C. Figure 13b shows the TGA curve of L1. Kraft lignin fractions were extracted from black liquor (a product of kraft pulping of softwood, mainly spruce and pine).

## 4. Materials and Methods

### 4.1 Isolation and Purification

Kraft lignin was extracted via gradual acidification of black liquor using HCl and H<sub>2</sub>SO<sub>4</sub> at specific pH, temperature, and time of stirring variations. Results of these precipitation conditions were investigated for yield; the optimum acidification was determined to be the one using H<sub>2</sub>SO<sub>4</sub> with stirring at room temperature and pH=2 for 90-180 min to get the first fraction of lignin (L1). L1 was soaked with diethyl ether to produce the second fraction (L2). Selective extraction using acetone produced L3 another selective extraction of L3 using ethanol produced L4. Diethyl ether was used as a precipitating solvent for the selective extractions. The purification was monitored by thin layer chromatography (TLC).

Organosolv lignins were prepared according to an earlier published procedure [32].

### 4.2 FTIR Analysis

FTIR spectra of the lignin samples were recorded on a Jasco FTIR 410 spectrometer in the range of 3800–500 cm<sup>-1</sup> using a KBr disc containing 1 % finely ground samples. The spectrum recorded over 30 scans with a resolution of 4 cm<sup>-1</sup>.

### 4.3 UV-Vis Analysis

UV-Vis spectra were recorded on a Hewlett-Packard 450 Diode Array spectrometer. The lignin UV-Vis absorption spectrum was obtained at room temperature using a sample (3.2 ml) containing 50 µg ml<sup>-1</sup> of KL in 0.1 M NaOH. The absorbance was measured in the range of 210–500 nm.

### 4.4 2D HSQC NMR Analysis

HSQC spectra were measured with 4 scans and 16 prior dummy scans. The data of 4k points were recorded with a spectral width of 7211 Hz, a receiver gain of 2050, and a total acquisition time of 0.28 s. O1 was set to 5 ppm (<sup>1</sup>H) and 80 ppm (<sup>13</sup>C).

### 4.5 31P NMR Analysis

<sup>31</sup>P NMR spectra were acquired using <sup>1</sup>H-<sup>31</sup>P decoupling experiment with 32 scans and 2 prior dummy scans. The data of 131k points were recorded with a spectral width of 12175.324 Hz, a receiver gain of 2050, and a total acquisition time of 5.38 s.

### 4.6 SEC Analysis

The lignin sample was completely dissolved in THF (1 mg mL<sup>-1</sup>) at room temperature with gentle stirring at room temperature. Size exclusion chromatography was performed at room temperature with THF as the mobile phase (flow rate 1.0 mL min<sup>-1</sup>) and an UV detector (254 nm) using an Agilent 1100 instrument.

#### 4.7 Pyrolysis GC-MS

Approximately 1 mg of lignin sample was inserted without further preparation into the bore of the pyrolysis solids injector and then placed with the plunger on the quartz wool of the quartz tube from the furnace pyrolyzer Pyrojector IITM (SGE Analytical Science, Melbourne, Australia). The pyrolyzer was operated at a constant temperature of 550 °C. The pressure of helium carrier gas at the inlet to the furnace was 95 kPa. The pyrolyzer was connected to a Trace 2000 gas chromatograph (ThermoQuest/CE Instruments, Milan, Italy) with a quadrupole mass spectrometer Voyager (ThermoQuest/Finnigan, MassLab Group, Manchester, UK) operated in electron impact ionization (EI) mode. A fused silica GC capillary column DB-5 ms 30 m long, 0.25 mm I.D., 0.25  $\mu$ m film thickness (J&W, Folsom, CA, USA) was used.

The gas chromatographic conditions were as follows: programmed temperature of the capillary column was from 60 °C (1 min hold) at 2.5 °C min<sup>-1</sup> to 100 °C and then 10 °C min<sup>-1</sup> to 280 °C (20 min hold at 280 °C). The temperature of the split/splitless injector was 250 °C and the split flow was 10 cm<sup>3</sup> min<sup>-1</sup>. Helium, grade 5.0 (Westfalen AG, Muenster, Germany) was used as a carrier gas at constant pressure of 70 kPa during the whole analysis. The transfer line temperature was 280 °C. The MS EI ion source temperature was kept at 250 °C. The ionization occurred with a kinetic energy of the impacting electrons of 70 eV. The current emission of the rhenium filament was 150  $\mu$ A. The MS detector voltage was 350 V. Mass spectra and reconstructed chromatograms (total ion current [TIC]) were obtained by automatic scanning in the mass range  $m/z$  35–455 u. Pyrolysis–GC/MS data were processed with the Xcalibur software (ThermoQuest) and the NIST 05 mass spectral library.

#### 4.8 TGA

TGA was performed with about 10 mg of lignin using a Netzsch TGA 209 F1 with a heating rate of 20 °C min<sup>-1</sup> under nitrogen atmosphere. The temperature ranged from ambient to 800 °C.

#### 4.9 DSC

Glass transition temperatures ( $T_g$ ) were determined using a Perkin Elmer 8000 differential scanning calorimeter. The scans were run from a starting temperature of 0 °C (held for 3 min) under a nitrogen flow rate of 10 mL min<sup>-1</sup>. The samples were then heated from 0 to 226 °C at 20 °C min<sup>-1</sup>. Before being tested, the samples were extensively dried for 24 h in an oven at 50 °C under vacuum.

#### 4.10 X-ray Diffraction

Powdered lignin samples were used for obtaining X-ray diffraction patterns. X-ray diffractograms with  $2\theta$ , ranging from 10 ° to 65 ° were collected with a Bruker D2 PHASER X-ray diffractometer (Germany) using Theta/Theta geometry with a secondary monochromator (CuK $\alpha$  radiation, 30 kV/10 mA, step 5407 in  $2\theta$ , 96 s/step).

#### 4.11 Total Phenol Content (TPC)

A volume of 2.5 mL Folin–Ciocalteu reactive and 5 mL of 20% Na<sub>2</sub>CO<sub>3</sub> solution were mixed with 0.5 mL of lignin solution (20 mg in 10 mL of DMSO). The mixture was kept for 30 min at 40 °C before measuring the absorbance at 750 nm. The intensity of blue color was measured at 750 nm in a UV–VIS spectrophotometer (Jasco V-630). The total phenols content was determined using a standard curve with gallic acid solutions.

#### 4.12 Antioxidant Activity

Spectrophotometric method based on the use of the free radical 2,2-diphenyl-1-picrylhydrazyl (DPPH) using a spectrophotometer Jasco V-630. Extracted samples dissolved in dioxane/water (90:10, v/v) at a concentration of 1 g/L; 0.1 mL of the sample solution was mixed with 3.9 mL of a 6  $\times$  10<sup>-5</sup> M DPPH solution, and the absorbance at 518 nm of the mixture was measured at 15 min and 30 min, respectively.

## 5. Conclusions

The status quo of antioxidant assays, their advantages and limitations were shortly summarized and compared. Results from antioxidant capacity studies using the DPPH assay were correlated to structure differences of various lignins. In detail, the influence of biomass source (beech *versus* spruce/pine), pulping (kraft *versus* organosolv) and purification degree of the isolated lignins on the antioxidant activity is discussed. A double-fold selective extraction was the most efficient purification procedure confirmed via UV-Vis, FTIR and HSQC NMR spectroscopy, SEC, and XRD analysis. Antioxidant activity measured via DPPH inhibition of kraft lignin fractions are above reported literature values, confirming that technical black liquor can be used without further modification. Storage of purification fractions decreased the TPC values and increased the DPPH inhibition.

**Acknowledgments:** Financial support via BMBF program “IngenieurNachwuchs” projects “LignoBau” (03FH013IX4); Bonn-Rhein-Sieg University/Graduate Institute for scholar ship (A.A., B.E.-H.) and Erasmus-Mundus Avempace-II scholar ship (A.A.); and North Carolina State University in conjunction with the DAAD RISE Scholarship Program (M.L.).

**Author Contributions:** A.A. mainly contributed to the manuscript, performed the experiments, analyzed the data and contributed main parts of the manuscript; B.E.-H. contributed analytical data; D.B. and M.L. performed antioxidant and TPC experiments and analyzed data; M.L. as native speaker contributed in writing; B.K. and S.W. contributed materials and analysis tools; M.S. conceived and designed the experimental studies and wrote the manuscript.

**Conflicts of Interest:** The authors declare no conflict of interest.

## References

1. Kamm, B.; Gruber, P.R.; Kamm, M. Biorefineries-Industrial Processes and Products. In *Ullmann's Encyclopedia of Industrial Chemistry*, Wiley-VCH, Weinheim, 2016, DOI:10.1002/14356007.l04\_l01.pub2.
2. Kamm, B.; Kamm, M.; Hirth, T.; Schulze, M. Lignocelluloses Based Chemical Products and Product Family Trees. In *Biorefineries – Industrial Processes and Products*, vol 2, Kamm, M., Kamm, B., Gruber, P.C. Eds., Wiley-VCH, Weinheim, 2006, pp 97-150, ISBN 3-527-31027-4.
3. Rinaldi R., Jastrzebski R., Clough M. T., Ralph J., Kennema M., Bruijninx P. C. A., Weckhuysen B. M. Paving the Way for Lignin Valorisation: Recent Advances in Bioengineering, Biorefining and Catalysis. *Angew. Chem. Int. Ed.* **2016**, 55, 2–54, DOI: 10.1002/anie.201510351.
4. Sipponen, M. H.; Farooq, M.; Koivisto, J.; Pellis, A.; Seitsonen, J.; Österberg, M. Spatially confined lignin nanospheres for biocatalytic ester synthesis in aqueous media. *Nature Comm.* **2018**, 9(1) DOI: 10.1038/s41467-018-04715-6.
5. Alzagameem, A.; El Khaldi-Hansen, B.; Kamm, B.; Schulze, M. Lignocellulosic biomass for energy, biofuels, biomaterials, and chemicals. In *Biomass and Green Chemistry*, 1<sup>st</sup> ed.; Vaz Jr, S. Ed.; Springer International Publishing, 2018, pp. 95-132, ISBN 978-3-319-66736-2, DOI:10.1007/978-3-319-66736-2.
6. Liu, Q.; Luo, L.; Zheng, L. Lignins: Biosynthesis and Biological Functions in Plants. *Int. J. Mol. Sci.* **2018**, 19, 335, DOI:10.3390/ijms19020335.
7. Nieminen K., Kuitunen S., Paananen M., Sixta H. Novel Insight into Lignin Degradation during Kraft Cooking. *Ind. Eng. Chem. Res.* **2014**, 53, 2614–2624, DOI:10.1021/ie4028928.
8. Løhre C., Halleraker H. V., Barth T. Composition of Lignin-to-Liquid Solvolysis Oils from Lignin Extracted in a Semi-Continuous Organosolv Process. *Int. J. Mol. Sci.* **2017**, 18, 225, 1-17, DOI:10.3390/ijms18010225.
9. Hundt, M.; Engel N.; Schnitzlein, K.; Schnitzlein, M.G. The AlkaPolP process: Fractionation of various lignocelluloses and continuous pulping within an integrated biorefinery concept. *Chem. Eng. Res. Design* **2016**, 107, 13-23, DOI: 10.1016/j.cherd.2015.10.013.
10. Pye, E. K. Industrial lignin production and applications. In *Biorefineries--Industrial Processes and Products*; Kamm B., Gruber P. R., Kamm M.; Wiley-VCH Verlag GmbH & Co. KGaA: Weinheim, Germany, 2006; Volume 2, pp165-200, ISBN: 978-3-527-31027-2.
11. Gou, M.; Ran, X.; Martin, D.W.; Liu, C.J. The scaffold proteins of lignin biosynthetic cytochrome P450 enzymes. *Nat. Plants* **2018**, 4, 299-310, DOI: 10.1038/s41477-018-0142-9.
12. Lupoi, J.S.; Singh, S.; Parthasarathi, R.; Simmons, B.A.; Henry, R.J. Recent innovations in analytical methods for the qualitative and quantitative assessment of lignin. *Renew. Sust. Energ. Rev.* **2015**, 49, 871-906, DOI:10.1016/j.rser.2015.04.091.

13. Sluiter, A.; Hames, B.; Ruiz, R.; Scarlata, C.; Sluiter, J.; Templeton, D.; Crocker, D. Determination of Structural Carbohydrates and Lignin in Biomass. Laboratory Analytical Procedure (LAP). Technical Report NREL/TP-510-42618. Issue Date: April 2008, Revision Date: August 2012 (Version 08-03-2012).
14. Lignin Market Analysis By Product (Lignosulphonates, Kraft Lignin, Organosolv Lignin) By Application (Macromolecules, Aromatics), By Region (North America, Europe, APAC, Central & South America, MEA), And Segment Forecasts, 2014 – 2025. ID: 4240413 Report, April 2017, Region: America, Europe, North America, United States, 110 pages, Grand View Research.
15. Lignin Market - Forecasts from 2018 to 2023. ID: 4479455. Report February 2018, 104 pages, Knowledge Sourcing Intelligence LLP.
16. Beisl, S.; Miltner, A.; Friedl, A. Lignin from Micro- to Nanosize: Production Methods. *Int. J. Mol. Sci.* **2017**, *18*, 1244, DOI:10.3390/ijms18061244.
17. Schutyser, W.; Renders, T.; Van den Bosch, S.; Koelewijn, S.F.; Beckham, G.T.; Sels, B.F. Chemicals from lignin: an interplay of lignocellulose fractionation, depolymerisation, and upgrading. *Chem. Soc. Rev.* **2018**, *47*, 852–908, DOI: 10.1039/c7cs00566k.
18. Aminzadeh S., Lauberts M., Dobeles G., Ponomarenko J., Mattsson T., Lindstroem M. E., Sevastyanova O. Membrane filtration of kraft lignin: Structural characteristics and antioxidant activity of the low-molecular-weight fraction. *Ind. Crop. Prod.* **2018**, *112*, 200–209, DOI: 10.1016/j.indcrop.2017.11.042.
19. Garrett, A.R.; Murray, B.K.; Robison, R.A.; O'Neill, K.L. Measuring Antioxidant Capacity Using the ORAC and TOSC Assays. In: Armstrong D. (Eds) *Advanced Protocols in Oxidative Stress II. Methods in Molecular Biology (Methods and Protocols)*, vol 594. 2010 Humana Press, Totowa, NJ. Online ISBN: 978-1-60761-411-1, DOI:10.1007/978-1-60761-411-1\_17.
20. Tai, A.; Sawano, T.; Yazama, F.; Ito, H. Evaluation of antioxidant activity of vanillin by using multiple antioxidant assays. *Biochim. Biophys. Acta* **2011**, *1810*, 170–177, DOI:10.1016/j.bbagen.2010.11.004.
21. Ponomarenko, J.; Dizhbite, T.; Lauberts, M.; Viksna, A.; Dobeles, G.; Bikovens, O.; Telysheva, G. Characterization of softwood and hardwood lignoblast kraft lignins with emphasis on their antioxidant activity. *BioResources* **2014**, *9*, 2051–2068, DOI: 10.15376/biores.9.2.2051-2068.
22. Benzie, I. F. and Devaki, M. (2017). The ferric reducing/antioxidant power (FRAP) assay for non-enzymatic antioxidant capacity: concepts, procedures, limitations and applications. In *Measurement of Antioxidant Activity & Capacity*, 1<sup>st</sup> ed.; Apak, R.; Capanoglu, E.; Shahidi, F.; Eds., John Wiley & Sons Ltd., 2017, chapter 5, Online ISBN: 9781119135388, DOI:10.1002/9781119135388.
23. Cano, A.; Arnao, M.B. ABTS/TEAC (2,2'-azino-bis(3-ethylbenzothiazoline-6-sulfonic acid)/Trolox@-Equivalent Antioxidant Capacity) radical scavenging mixed-mode assay. In *Measurement of Antioxidant Activity & Capacity*, 1<sup>st</sup> ed.; Apak, R.; Capanoglu, E.; Shahidi, F.; Eds., John Wiley & Sons Ltd., 2017, chapter 7, Online ISBN: 9781119135388, DOI:10.1002/9781119135388.
24. Özyürek, M.; Güclü, K.; Tütem, E. *et al.* A comprehensive review of CUPRAC methodology. *Anal. Methods*, **2011**, *3*, 2439–2453, DOI:10.1039/C1AY05320E.
25. Mishra, K.; Ojha, H.; Chaudhury, N.K. Estimation of antiradical properties of antioxidants using DPPH assay: A critical review and results. *Food Chem.* **2011**, *130*, 1036–1043, DOI:10.1016/j.foodchem.2011.07.127.
26. Sanchez-Rangel, J.C.; Benavides, J.; Heredia, J.B.; Cisneros-Zevallos, L.; Jacobo-Velázquez, D.A. The Folin-Ciocalteu assay revisited: improvement of its specificity for total phenolic content determination. *Anal. Methods* **2013**, *5*, 5990–5999, DOI:10.1039/C3AY41125G.
27. Witzler, M.; Alzagameem, A.; Bergs, M.; El Khaldi-Hansen, B.; Klein, S.E.; Hielscher, D.; Kamm, B.; Kreyenschmidt, J.; Tobiasch, E.; Schulze, M. Lignin-Derived Biomaterials for Drug Release and Tissue Engineering. *Molecules* **2018**, *23*, 1885, DOI:10.3390/molecules23081885.
28. Shivakumar, A.; Kumar, M.S.Y. Critical Review on the Analytical Mechanistic Steps in the Evaluation of Antioxidant Activity. *Critical Rev. Anal. Chem.* **2018**, *48*, 214–236, DOI: 10.1080/10408347.2017.1400423.
29. Dizhbite, T.; Telysheva, G.; Jurkane, V.; Viesturs, U. Characterization of the radical scavenging activity of lignins—natural antioxidants. *Biores. Technol.* **2004**, *95*, 309–317, DOI:10.1016/j.biortech.2004.02.024.
30. Santos, P.; Erdocia, X.; Gatto, D.A.; Labidi, J. Characterisation of Kraft lignin separated by gradient acid precipitation. *Ind. Crops Prod.* **2014**, *55*, 149–154, DOI: 10.1016/j.indcrop.2014.01.023.
31. Aminzadeh, S.; Lauberts, M.; Dobeles, G.; Ponomarenko, J.; Mattsson, T.; Lindstroem, M. E.; Sevastyanova, O. Membrane filtration of kraft lignin: Structural characteristics and antioxidant activity of the low-molecular-weight fraction. *Ind. Crops Prod.* **2018**, *112*, 200–209, DOI:10.1016/j.indcrop.2017.11.042.

32. Hansen, B.; Kamm, B.; Schulze, M. Qualitative and quantitative analysis of lignin produced from beech wood by different conditions of the Organosolv process. *J. Polym. Environ.* **2016**, *24*, 85–97, DOI:10.1007/s10924-015-0746-3.
33. Hansen, B.; Kamm, B.; Schulze, M. Qualitative and quantitative analysis of lignins from different sources and isolation methods for an application as a biobased chemical resource and polymeric material. In *Analytical Techniques and Methods for Biomass Products*. Vaz Jr, S., Seidl, P., Eds., Springer, 2017, pp. 15–44, ISBN 978-3-319-41414-0, DOI:10.1007/978-3-319-41414-0.
34. Fițișău, I.F.; Peter, F.; Boeriu, C.G. Structural Analysis of Lignins from Different Sources. *World Academy Sci. Eng. Technol.* **2013**, *76*, 107–112.
35. Vivekanand, V.; Chawade, A.; Larsson, M.; Larsson, A.; Olsson, O. Identification and qualitative characterization of high and low lignin lines from an oat TILLING population. *Ind. Crops Prod.* **2014**, *59*, 1–8, DOI:10.1016/j.indcrop.2014.04.019.
36. Azadi, P.; Inderwildi, O.R.; Farnood, R.; King, D.A. Liquid fuels, hydrogen and chemicals from lignin: A critical review. *Renew. Sust. Energ. Rev.* **2013**, *21*, 506–523, DOI: 10.1016/j.rser.2012.12.022.
37. Gilca, I.A.; Ghitescu, R.E.; Puitel, A.C.; Popa, V.I. Preparation of lignin nanoparticles by chemical modification. *Iran. Polym. J.* **2014**, *23*, 355–363, DOI: 10.1007/s13726-014-0232-0.
38. Sun, S.-N.; Cao, X.-F.; Xu, F.; Sun, R.-C.; Jones, G.L. Structural Features and Antioxidant Activities of Lignins from Steam-Exploded Bamboo (*Phyllostachys pubescens*). *J. Agric. Food Chem.* **2014**, *62*, 5939–5947, DOI: 10.1021/jf5023093.
39. Sulaeva, I.; Zinovyev, G.; Plankeele, J.M.; Sumerskii, I.; Rosenau, T.; Potthast, A. Fast Track to Molar Mass Distributions of Technical Lignins. *ChemSusChem* **2017**, *10*, 629–635, DOI:10.1002/cssc.201601517.
40. Monakhova, Y.; Diehl, B.W.K.; Do, X.T.; Witzleben, S.; Schulze, M. Novel method for the determination of average molecular weight of natural polymers based on 2D DOSY NMR and chemometrics: example of heparin. *J. Pharm. Biomed. Anal.* **2018**, *149*, 128–132, DOI:10.1016/j.jpba.2017.11.016.
41. Zhao, S.; Liu, M.; Zhao, L.; Zhu, L. Influence of Interactions among Three Biomass Components on the Pyrolysis Behavior. *Ind. Eng. Chem. Res.* **2018**, *57*, 5241–524, DOI: 10.1021/acs.iecr.8b00593.
42. Vallejos, M.E.; Felissia, F.E.; Curvelo, A.A.S.; Zambon, M.D.; Ramos, L.; Area, M.C. Chemical and physico-chemical characterization of lignins obtained from ethanol-water fractionation of bagasse. *BioResources* **2011**, *6*, 1158–1171.
43. Ramezani, N.; Sain, M. Thermal and Physiochemical Characterization of Lignin Extracted from Wheat Straw by Organosolv Process. *J. Polym. Environ.* **2018**, *26*, 3109–3116, DOI: 10.1007/s10924-018-1199-2.
44. Garcia, A.; Toledano, A.; Serrano, L.; Egues, I.; Gonzalez, M.; Marin, F.; Labidi, J. Characterization of lignins obtained by selective precipitation. *Sep. Pur. Technol.* **2009**, *68*, 193–198, DOI: 10.15376/biores.11.4.9869-9879.
45. Singh, M.; Jha, A.; Kumar, A.; Hettiarachchy, N.; Rai, A.K.; Sharma, D. Influence of the solvents on the extraction of major phenolic compounds (punicalagin, ellagic acid and gallic acid) and their antioxidant activities in pomegranate aril. *J. Food Sci. Technol.* **2014**, *51*, 2070–2077, DOI: 10.1007/s13197-014-1267-0.
46. Akowuah, G.A.; Ismail, Z.; Norhayati, I.; Sadikun, A. The effects of different extraction solvents of varying polarities on polyphenols of *Orthosiphon stamineus* and evaluation of the free radical-scavenging activity. *Food Chem.* **2005**, *93*, 311–317, DOI: 10.1016/j.foodchem.2004.09.028.
47. Felicio, C.M.; da Hora Machado, A.E.; Castellan, A. Routes of degradation of  $\beta$ -O-4 syringyl and guaiacyl lignin model compounds during photobleaching processes. *J. Photochem. Photobiol. A: Chem.* **2003**, *156*, 253–265, DOI:10.1016/S1010-6030(03)00007-8.
48. Do, X.T.; Nietzsche, A.; Jung, C.; Witzleben, S.; Schulze, M. Lignin-Depolymerisation via UV-Photolysis and Titanium Dioxide Photocatalysis. *Preprints* **2017**, 2017100128, DOI:10.20944/preprints201710.0128.v1).